Metal−Polymer Composites: Synthesis and Characterization of Polyaniline and Other Polymer@Silver Compositions

Guy Nesher, Gad Marom,* and David Avnir*

Institute of Chemistry, The Hebrew University of Jerusalem, Jerusalem 91904, Israel

Received March 6, 2008. Revised Manuscript Received April 17, 2008

A method was developed for the entrapment of water-insoluble hydrophobic polymers in a metallic matrix, thus generalizing further the routes for obtaining the novel organics@metal composite materials. The reaction took place in an organic phase using the reduction of metal ions by DMF in the presence of water. The reductive entrapment of polyaniline was studied in detail using XRD, SEM, BET, TGA, UV−vis, XPS, and density measurements, and the mechanism of the entrapment was established. The scope of this approach is demonstrated by entrapment of two additional hydrophobic polymers, polystyrene and polyacrylonitrile.

Introduction

Whereas the number of metal elements is small and limited, that of organic and biological molecules is vast and virtually unlimited. Naturally, hybridization of these two parent families can enrich the property library and widen the application scope offered by each of them individually. Recently, this principle has been behind a series of studies[1–6] that introduced a new family of materials, designated as organic compound-doped metals. The methodology of their preparation enables one to incorporate small or large (polymeric) organic molecules within metals, thus creating a new family of metal matrix composites. Various useful applications have been already demonstrated, such as formation of metallic catalysts[5] and induction of unusual properties to metals, such as acidity[1] and chirality in bulk gold and silver.[2] The methodology of preparation of those metal matrix composites involves metal synthesis by chemical reduction of a metal cation in the presence of the selected organic molecule. The reductive entrapment can be carried out either homogenously,[1–4] with water-soluble reducing agents, or heterogeneously,[6] with a powder of metal. Most of our studies have been carried out on copper, silver, and gold, for which a variety of metal salts can be used. The composite is obtained in a powder form, which can be hot pressed to create films or discs.

Special attention has been devoted in our studies to the entrapment of polymers because intimate polymer@metals composites represent novel materials, which, to the best of our knowledge, have not been presented before. Thus far, water-soluble polymers could be entrapped because the of the aqueous reduction conditions. Thus prepared were poly(styrenesulphonic acid)@Ag, poly(vinylalcohol)@Ag, poly(vinylbenzyltrimethylammonium hydroxide)@Ag, Nafion@Ag, Nafion@Cu, and Nafion@Au. However, since most of the widely used polymers are hydrophobic and in order to enlarge the family of polymer@metal composites to encompass these additional polymers, a new entrapment methodology is required.

Scheme 1. Reduction Reaction of Silver Ions by DMF

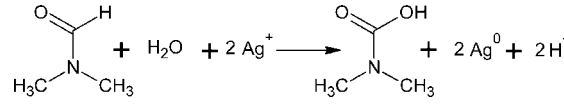

Of the various reduction processes of metal cations in an organic phase,[7–12] one method emerged as particularly attractive, namely, use of *N*,*N*-dimethylformamide (DMF) due of its dual action. DMF is an excellent solvent for many polymers ("good solvent"), while at the same time it is a potent reducing agent for some metal cations.[13] Its activity can be triggered at will by adding an equimolar amount of water (small enough not to affect the dissolution properties) according to Scheme 1.

The main focus of this study is the entrapment of electrically semiconductive polyaniline (PANI) in silver, for which detailed analyses are presented and a mechanism of entrapment is established. Furthermore, the commonalty of the method is proven by showing its applicability to two other polymers, namely, polyacrylonitrile (PAN) and polystyrene (PS). Whereas PAN can be converted to a semiconductive conjugated "ladder" polymer via polymerization of

* Corresponding author. gadm@vms.huji.ac.il (G.M.); david@chem.ch.huji.ac.il (D.A.).

(1) Behar-Levy, H.; Avnir, D. *Adv. Funct. Mater.* **2005**, *15*, 1141.
(2) Behar-Levy, H.; Neumann, O.; Naaman, R.; Avnir, D. *Adv. Funct. Mater.* **2007**, *19*, 1207.
(3) Behar-Levy, H.; Avnir, D. *Chem. Mater.* **2002**, *14*, 1736.
(4) Behar-Levy, H.; Shter, G. E.; Grader, G. S.; Avnir, D. *Chem. Mater.* **2004**, *16*, 3197.
(5) Shter, G. E.; Behar-Levy, H.; Gelman, V.; Grader, G. S.; Avnir, D. *Adv. Funct. Mater.* **2007**, *17*, 913.
(6) Yosef, I.; Avnir, D. *Chem. Mater.* **2006**, *18*, 5890.
(7) Huang, Z. Y.; Mills, G.; Hajek, B. *J. Phys. Chem.* **1993**, *97*, 11542.
(8) Sun, Y.; Xia, Y. *Science* **2002**, *298*, 2176.
(9) Zhu, H.; Zhang, C.; Yin, Y. *J. Cryst. Growth* **2004**, *270*, 722.
(10) Condorelli, G. G.; Costanzo, L. L.; Fragala, I. L.; Giuffrida, S.; Ventimiglia, G. *J. Mater. Chem.* **2003**, *13*, 2409.
(11) Kapoor, S.; Mukherjee, T. *Chem. Phys. Lett.* **2003**, *370*, 83.
(12) Joshi, S. S.; Patli, S. F.; Iyer, I.; Mahumuni, S. *Nanostruct. Mater.* **1998**, *10*, 1135.
(13) Pastoriza-Santos, I.; Liz-Marzan, L. *Pure Appl. Chem.* **2000**, *72*, 83.

10.1021/cm800657j CCC: $40.75
Published on Web 06/11/2008

Scheme 2. Structure of Polyacrylonitrile (a) and the Polymerization Process which Takes Place Above 180 °C and Creates a Ladder Polymer (b)

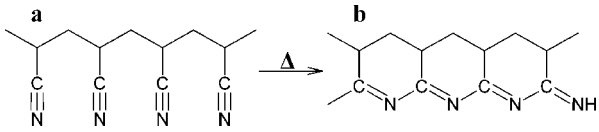

its pending nitrile groups (Scheme 2) (a process which takes place above 180 °C[14,15] or at lower temperatures in the presence of metal cations[16]), PS is unaffected by the reaction.

Experimental Section

Chemicals. Polyaniline (PANI, emeraldine base, $M_w \approx 100\,000$) and $AgNO_3$ were from Aldrich. Polyacrylonitrile (PAN, $M_w \approx 150\,000$) and monocarboxy-terminated-polystyrene (PS, $M_w \approx 150{,}000$) were from Scientific Polymer Products, NY. Silver nanoparticles (<100 nm, 99.5%) were from Sigma.

Entrapment Procedure of PANI. To a hot stirred solution of 50 mL of DMF, 0.1 g (0.0009 mol of monomers) of PANI was added, and after 1 min 1.70 g of $AgNO_3$ (0.01 mol) was added as well. The combined solution was heated to 100 °C and stirred for 2 h, after which 5.0 mL (0.25 mol) of distilled water was added. The reduction, which begins immediately with addition of water and is clearly apparent, was carried out overnight, forming PANI@Ag. The precipitate was filtered and washed with two portions of 10 mL of DMF and one portion of 10 mL of water and dried under vacuum for a few hours. The resulting material, 1.0 g of PANI@Ag, contained ~95% of the initial polymer used in the reaction mixture, as determined by TGA. The yield with respect to the $AgNO_3$ is ~90%, and the color of the silver was changed by the presence of the polymer into gray black.

Entrapment Procedure of PAN. To a hot and stirred solution solution of 50 mL of DMF, 0.1 g of PAN (0.0015 mol of monomers) was added, and after 15 min 1.70 g of $AgNO_3$ (0.01 mol) was added as well. The reaction between PAN and silver ions begins immediately,[16] and the solution turns black after 1 day. The combined solution was stirred for another 3 days, after which 5.0 mL (0.25 mol) of distilled water was added. Precipitation of PAN@Ag (black material, Figure 1c) begins after addition of water, and the reduction/entrapment reaction was continued overnight. The precipitated PAN@Ag was filtered and washed with 2 portions of 10 mL of DMF and one portion of 10 mL of water and dried under vacuum for a few hours. The resulting material, 0.8 g, contained ~79% of the initial polymer used in the reaction mixture, as determined by TGA. The yield with respect to $AgNO_3$ is ~85%.

Entrapment Procedure of PS. To 20 mL of toluene, 0.1 g of monocarboxy-terminated-PS (0.001 mol of monomers) was added under stirring. After 15 min, a solution of 1.70 g of $AgNO_3$ (0.01 mol) in 30 mL of DMF was added. After mixing the stirred solution remains clear. The flask was covered (to limit reduction of the silver ions before addition of the water) and stirred overnight (to enhance interaction between the PS molecules and the silver ions, probably through the carboxy group). The next day the solution was heated to 80 °C for 2 h, and then 1.0 mL (0.05 mol) of distilled water was added gently to the solution. Great care should be taken not to have phase separation during addition of water. Precipitation of PS@Ag (gray material) begins after addition of water, and the reduction/entrapment reaction was continued overnight. The precipitated PS@Ag was filtered and washed with one portion of 10 mL of toluene and one portion of 10 mL of DMF and dried under vacuum for a few hours. The resulting material, 0.6 g, contained ~35% of the initial polymer used in the reaction mixture, as determined by TGA. The yield with respect to $AgNO_3$ is ~70%.

Adsorption vs Entrapment. Adsorption and entrapment are distinctly different processes. For their comparison, the following experiments were carried out: The pure metal was prepared as described above except for the presence of the organic material. The amount adsorbed was determined by UV−vis spectroscopy of the filtered solution, where 0.1 g of PANI and 1 g of metallic Ag were stirred in the reaction conditions. The same adsorption experiment was done also with commercially available metal nanoparticles, and the amount absorbed was determined by UV−vis spectroscopy of the filtered solution.

Extraction Tests. In the case of PAN and PANI, extraction tests of the entrapped polymers into either DMF or DMSO were carried out by stirring 0.1 g of the product with 15.0 mL of solvent overnight. In the case of PS, the same extraction test was carried out in toluene.

Instrumentation. UV−vis absorption spectroscopy was carried out with a Hewlett-Packard 8452A diode-array UV−vis spectrophotometer. XRD measurement were carried out with Philips automated powder diffractometer (with PW1830 generator, PW1710 control unit, PW1820 vertical goniometer, 40 KV, 35 mA, Cu Kα (1.5405 Å)). SEM was carried on a Sirion (FEI) HR-SEM instrument (operating voltage is indicated for each picture). Thermogravimetric thermal analysis (TGA) was preformed on a Mettler TC10A/TC15 TA controller from 25 to 600 °C at a heating rate of 10 °C/min in flowing dry air. For a more exact analysis of the TGA graphs, the derivative weight loss was calculated using the supplied software. Surface area and porosity were determined from nitrogen adsorption/desorption isotherms with a Micromeritics ASAP-2020 physisorption instrument using the Brunauer−Emmett−Teller (BET) equation to characterize the overall surface area and the Barret−Joyner−Hallender (BJH) equation to determine the surface area in the mesoporous region. Density was determined from weight/volume analysis using a Micromeritics AccuPyc 1340 gas pycnometer instrument using helium as a displacing gas. The XPS (X-ray photoelectron spectroscopy) measurements were performed on a Kratos Axis Ultra X-ray photoelectron spectrometer. Spectra were acquired with a monochromated Al Kα (1486.7 eV) X-ray source with a 0° takeoff angle. The pressure in the test chamber was maintained at 1.5×10^{-9} Torr during the acquisition process. High-resolution XPS scans were collected for N 1s, C 1s, O 1s, and Ag 3d peaks with a pass energy of 20 eV and a step size of 0.1 eV. Data analysis and processing were performed with Vision processing data reduction software (Kratos Analytical Ltd.) and CasaXPS (Casa Software Ltd.).

Results and Their Interpretations

I. Characterization of PANI@Ag. Figure 1a and 1b shows that introduction of the polymer has changed the appearance of silver. While the undoped metal, made in the same way, takes the classical form of a silvery gray and dense spherical granules (Figure 1a), PANI@Ag is a grayish black powder (Figure 1b). The SEM photos (Figure 2) confirm these observations, showing the dense and nonporous pure silver (Figure 2a) and the nanosize particles (100−300 nm) of PANI@Ag (Figure 2b). The density of the pure silver

(14) Vaisman, L.; Larin, B.; Davidi, I.; Wachtel, E.; Marom, G.; Wagner, H. D. *Composites A* **2007**, *38*, 1354.
(15) Brokman, A.; Weger, M.; Marom, G. *Polymer* **1980**, *21*, 1114.
(16) Wang, Y.; Yang, Q.; Shan, G.; Wang, C.; Du, J.; Wang, S.; Li, Y.; Chen, X.; Jing, X.; Wei, Y. *Mater. Lett.* **2005**, *59*, 3046.

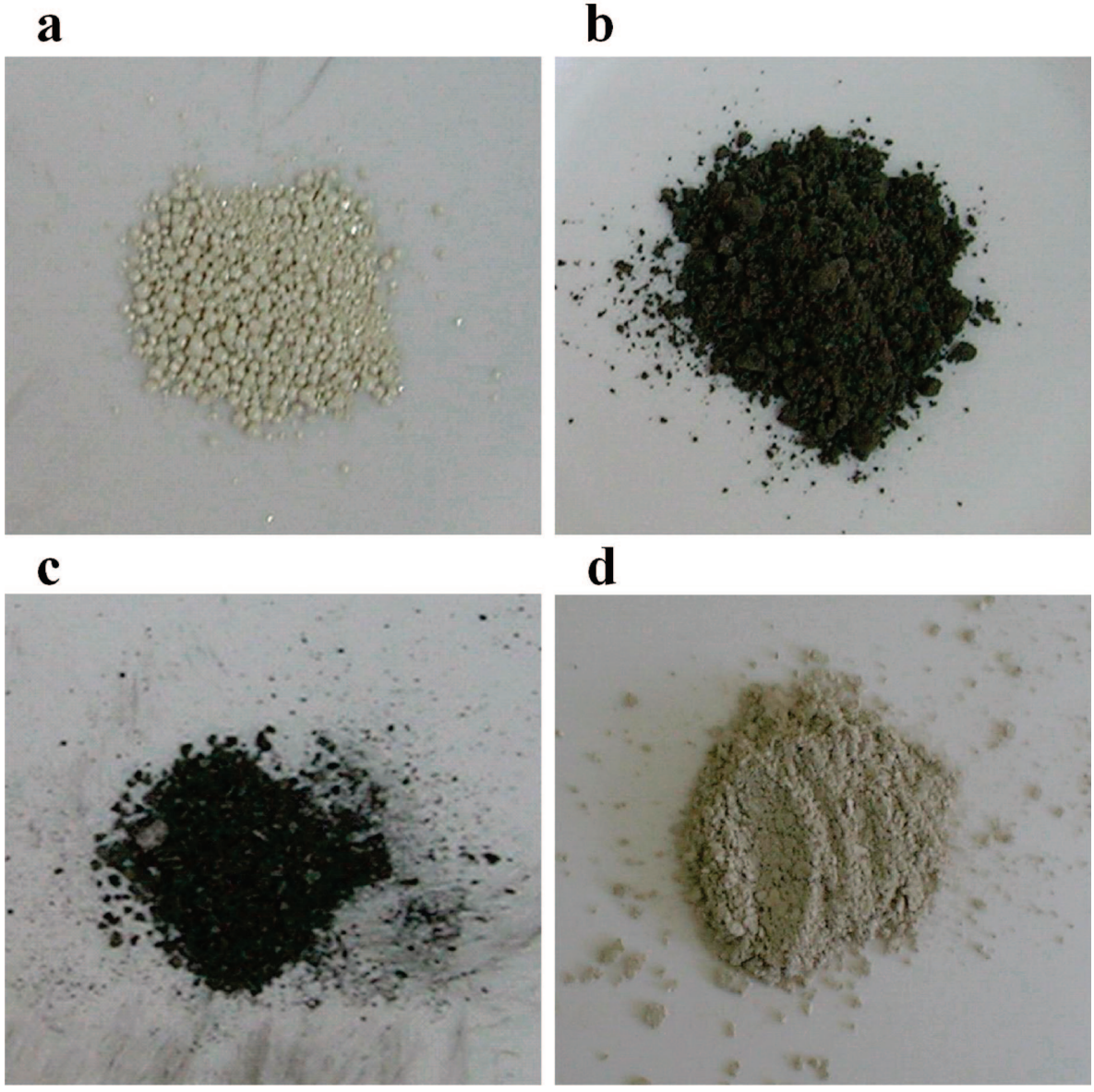

Figure 1. Macroscopic view of the products: (a) Ag, (b) PANI@Ag, (c) PAN@Ag, (d) PS@Ag.

spheres (Table 1) is high (10.4 g/mL) and close to the density of crystalline bulk Ag. The composite exhibits significantly lower density (~7.2 g/mL), reflecting both the contribution of the organic component and the interstitial porosity between the nanocrystals that form the bulk material. N_2 adsorption−desorption BET experiments (Table 2 and Figure 3) provide additional supportive data which confirm the visual observations and density measurements. A significant surface area (N_2−BET) increase from pure Ag to the composite can be seen, indicating higher porosity, or in fact, mesoporosity, as indicated by the high location of the P/P° hysteresis loops (Figure 3a). (It is noted though that this mesoporosity is considered low compared to those of classical adsorbents in the hundreds of m^2/g range, such as silica materials). Moreover, the excellent fit of the experimental values and the BET equation (Figure 3c) reflects a high level of adsorption site homogeneity, which in turn points to a high uniformity of the composite material. Finally, XRD analysis (Table 3) shows clearly that the metallic component of PANI@Ag comprises crystalline *FCC* Ag and that doping does not interfere with this structure. The characteristic diffraction lines of the metal remain unchanged, while no peaks of silver salts or silver oxide can be seen. Application of the Scherrer equation with the width of the diffraction peak at half-height[17] indicates that the elementary building block of the aggregated silver nanocrystals is in the ~40 nm size range, compared with ~60 nm of pure silver. We attribute the size reduction to growth restriction by the 'surfactant-like' interaction between the polymer and the granule.

Several observations were made with TGA. Figure 4 presents weight loss traces and their corresponding first derivatives for three composites. It is seen (Figure 4a) that the loading of the entrapped PANI is 8.5 wt %, which based on the densities (10.5 and 1.2 g/cm^3 for silver and PANI, respectively) amounts to 44 vol %. In terms of the atomic concentration,[18] the concentration of the organic fraction is 50 atom %, which, excluding the hydrogen atoms, reduces to 35 atom %. It is noted that the

(17) Cullity, B. D. *Elements of X-Ray Diffraction*, 2nd ed.; Addison-Wesley: Reading, MA, 1978.
(18) Shacham-Diamand, Y.; Inberg, A.; Sverdlov, Y.; Bogush, V.; Croitoru, N.; Moscovich, H.; Freeman, A. *Electrochem. Acta* **2003**, *48*, 2987.

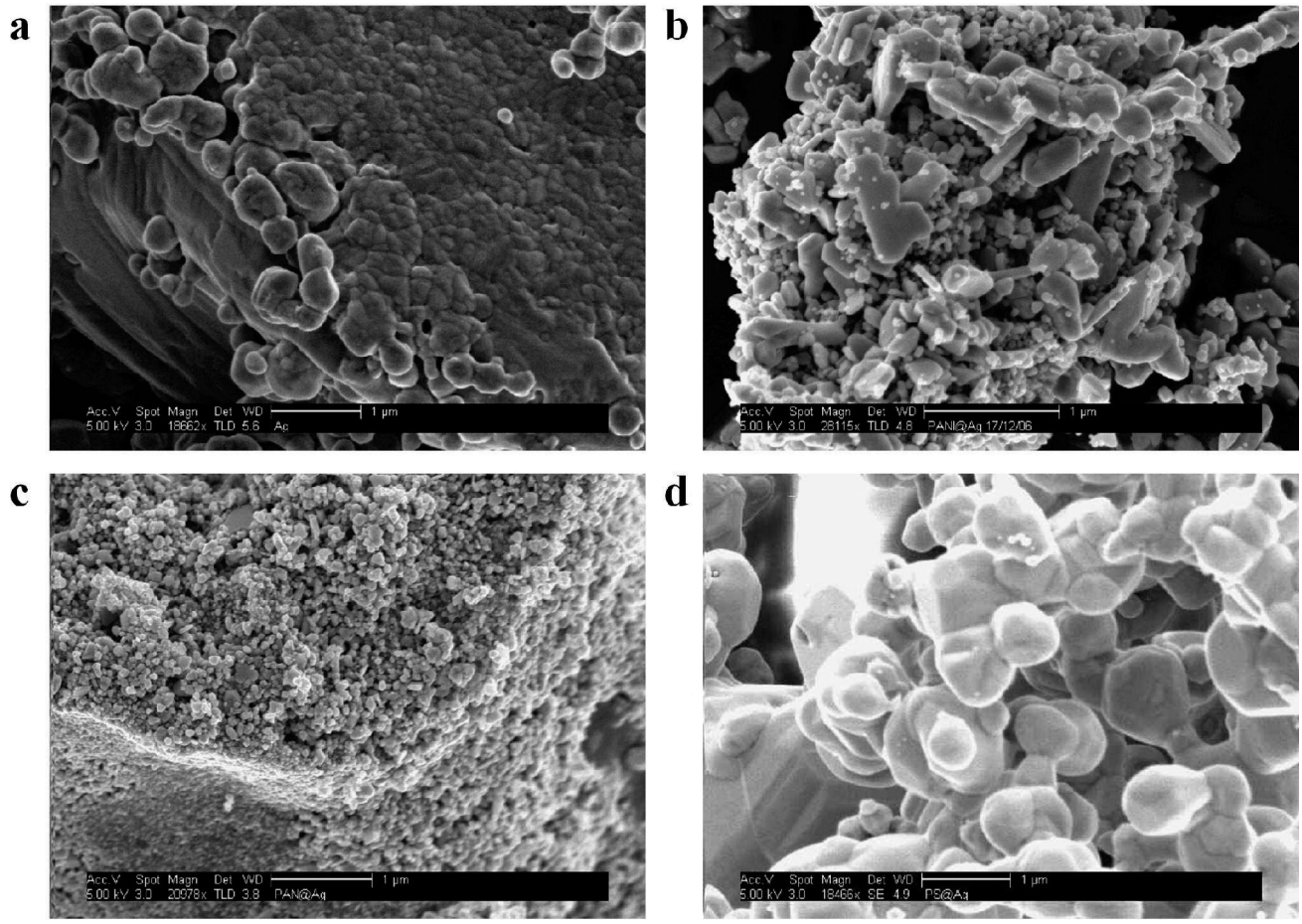

Figure 2. High-resolution SEM images: (a) Ag, (b) PANI@Ag, (c) PAN@Ag, (d) PS@Ag.

Table 1. Typical Densities of the Metal−Polymer Composites

sample	density (g/ml)
PANI@Ag	7.2
PAN@Ag	6.6
PS@Ag	8.6
Ag	10.4
Bulk Ag[a]	10.5

[a] *CRC Handbook of Chemistry and Physics*, 81st ed.

Table 2. Typical Surface Area and Pore Size Values

sample	BET, surface area (m^2/g)	BJH, pore volume (ml/g)	BJH, pore size (nm)
PANI@Ag	4.4	0.03	19
PAN@Ag	8.6	0.04	21
PS@Ag	0.05	0.0002	135
Ag	0.003		

entrapment level (including hydrogen atoms) is much higher than in previously reported polymer@metal composites, where it ranged from less than 1^4 to 25 atom %.[6] Also, the efficiency of the entrapment process was quite high, wherein 95% of the original PANI ended up in the composite material. The fact that occlusion of the polymeric phase in the metallic matrix is mainly by entrapment and not by adsorption is corroborated by the results in Table 4. It is seen that compared with the very low adsorption capacity of metallic Ag the overall entrapment is huge.

The second observation made by TGA refers to the catalytic nature of Ag in oxidation reactions,[19] revealed by the first derivative of the TGA trace. The polymer in the composites decomposes at a much lower temperature than the polymer in its free form (Figure 4d), namely, the decomposition peak of PANI in its free form is ~500 °C, whereas that of PANI in the composite is below 300 °C. This is accompanied by narrowing the decomposition range to less than 200 °C. Both effects reflect the catalytic action of metallic Ag in facilitating the oxidative decomposition.

II. Entrapment Effect on the Redox Forms of PANI. We recall that PANI in its base form consists of two main structural units, i.e., the benzoid diamine and quinoid diamine, shown in Scheme 3.[20] The fully oxidized and reduced forms contain only quinoid diamine (pernigraniline) and benzoid diamine (leucoemeraldine) units, respectively. The relative contents of these units, designated redox forms, express intermediate oxidation states, of which the 50:50 randomly distributed composition (emeraldine), used in this study, is noted. On the basis of a number of experimental indications it is concluded that the main form of the entrapped PANI is leucoemeraldine, implying that the entrapment process entails reduction of the original emeraldine. The first indication comes from the XPS analysis carried out on emeraldine and PANI@Ag. In emeraldine, a broad peak for N 1s is obtained (Figure 5a), which can be deconvoluted into two N 1s peaks with binding energies of

(19) Li, W. S.; Stampfl, C.; Scheffler, M. *Phys. Rev. Lett.* **2003**, *90*, 256102.
(20) Wei, Y.; Hsueh, K.; Jang, G. W. *Macromolecules* **1994**, *27*, 518.

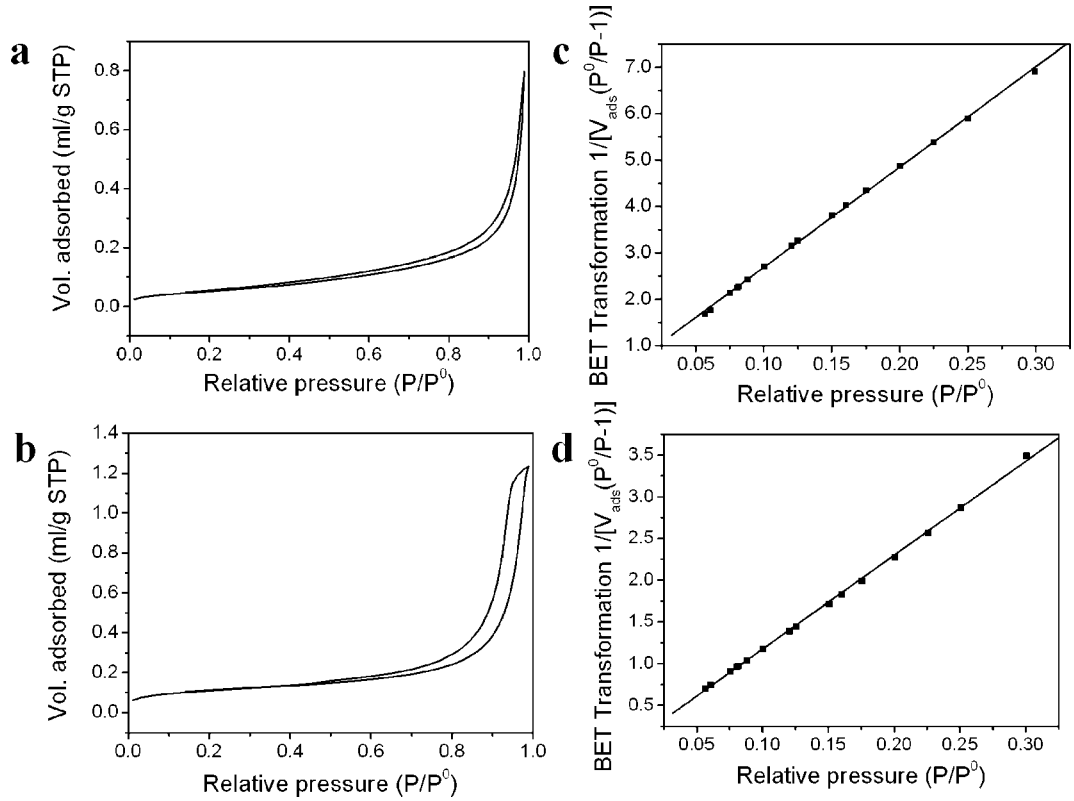

Figure 3. Adsorption−desorption BET isotherms of N_2 for (a) PANI@Ag and (b) PAN@Ag, and the compliance to the BET equation of (c) PANI@Ag and (d) PAN@Ag.

Table 3. X-ray Diffraction Patterns and Crystallite Size

	lit. data Ag[a]		Ag bulk		PANI@Ag		PAN@Ag	
plane (*hkl*)	Int	*d*(Å)	Int	*d*(Å)	Int	*d*(Å)	Int	*d*(Å)
111	100	2.359	1870	2.36	2080	2.36	720	2.36
200	40	2.044	840	2.04	625	2.04	222	2.04
220	25	1.445	430	1.44	450	1.44	188	1.44
crystallite size[b](nm)			59.7		43.3		27.8	

[a] 2003 JCPDS - International Center for Diffraction Data. [b] Calculated from the XRD patterns using Scherrer's equation.[17]

398.8 and 399.9 eV, assigned to neutral imine [═N−] and amine [−NH−] nitrogen atoms, respectively.[21,22] This results in a relative proportion of the quinoid and benzoid forms of 23% and 77%, respectively. In PANI@Ag, most of the quinoid form is reduced upon entrapment, as expressed by the dominating [−NH−] peak at 399.8 eV (96.7%) of the deconvoluted spectrum (Figure 5b). The new peak at 402.2 eV is attributed to an oxidized state of the nitrogen produced during the entrapment process.

Confirmation of these observations comes from the analysis of the filtered supernatant solution at the end of the entrapment reaction, which contained 5% of the original PANI. UV−vis measurements (Figure 6), considering the ratio of the 320 and 630 nm peaks of the benzoid and quinoid forms, respectively, show that the original ratio of 1.6 in the emeraldine[20] now increases to 8.3, compared with over 15 for the reduced PANI−leucoemeraldine form.[20] Furthermore, the results in Figure 6 show that adsorption of PANI onto silver particles did not affect the redox state of the adsorbed polymer, showing that entrapment and adsorption are distinctly different processes.

It is proposed that reduction of the quinoid diamine units during the entrapment reaction occurs via the electrochemical Ostwald ripening reaction[23,24] and formation of the silver nanoparticles. Indeed, recent studies showed that the standard electrode potential of a nanosize metal particle (E_p^0) differs from that of the bulk (E_{bulk}^0) and shifts to more negative values as

$$E_p^0 = E_{bulk}^0 - \frac{2\gamma v_M}{zFr} \quad (1)$$

where, ϑ_M is the molar volume, γ is the surface tension, z is the lowest valence state, F is Faraday's constant, and r is the particle radius. It is seen that E_p^0 decreases with r; in fact, the $1/r$ dependence enhances the effect quite significantly for very small r values. This implies that nanoparticles are more effective reducing agents than the bulk metal. However, because of the sharp $1/r$ dependence, most of the PANI reduction reaction will occur at the very early stages by nascent Ag particles. This is confirmed by the UV−vis spectra in Figure 6, wherein the results of the entrapment reaction are compared with those of two emeraldine−Ag suspensions. The heights of the 630 nm peaks reveal that the effect obtained by decreasing the Ag particle size to the nanometric range is significant, underlining the size effect on the reduction reaction. Apparently, this effect is enhanced further through the entrapment reaction which generates nascent Ag particles.

(21) Lui, X. X.; Bian, L. J.; Zhang, L. J. *J. Solid State Electrochem.* **2007**, *11*, 1279.
(22) Chen, Y.; Kang, E. T.; Neoh, K. G. *Appl. Surf. Sci.* **2002**, *185*, 267.
(23) Jiang, Q.; Liang, L. H.; Zhao, D. S. *J. Phys Chem. B* **2001**, *105*, 6275.
(24) Redmond, P. L.; Hallock, A. J.; Brus, L. E. *Nano Lett.* **2005**, *5*, 131.

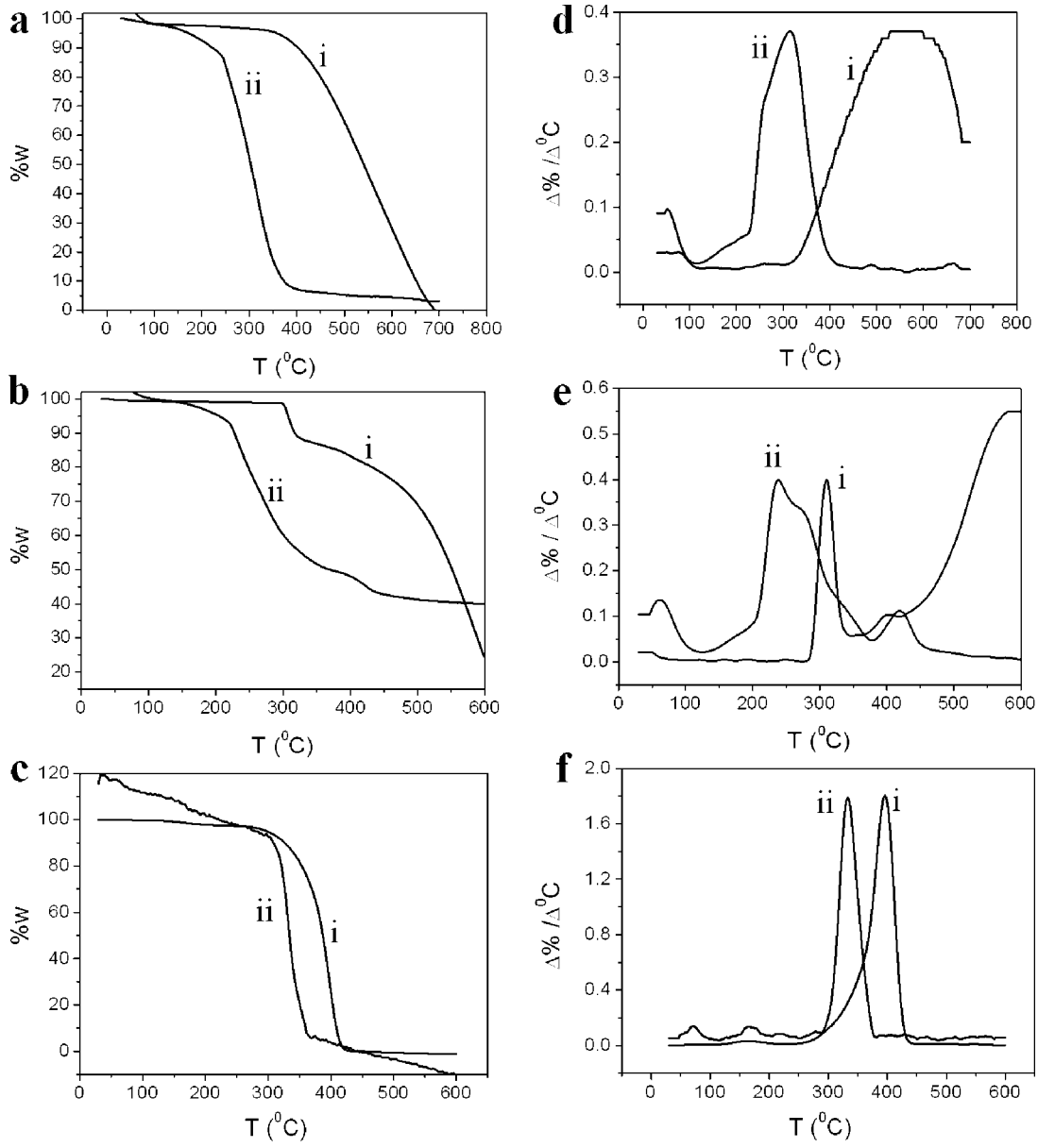

Figure 4. Thermogravimetric analysis in air of the original polymer (i) and the entrapped polymer (ii): (a) PANI vs PANI@Ag and (b) PAN vs PAN@Ag. First derivative (DTG) of (c) PANI vs PANI@Ag and (d) PAN vs PAN@Ag.

Table 4. Absorption vs Entrapment

sample	adsorption (%)	entrapment (%)
PANI@Ag	7	95
PAN@Ag	6	79
PS@Ag	1	25

III. Proposed Mechanism for PANI@Ag Formation. On the basis of the observations above, a mechanism for entrapment of PANI in silver can be proposed by the scheme in Figure 7. From the reaction equation (Scheme 1) it is clear that the reduction reaction is triggered by water addition. Yet, the TGA results (Figure 8) indicate that the polymer already interacts with the metal cation prior to the onset of the reaction and metal particle formation. This indication is based on the catalytic effect of the silver on the oxidative degradation. It is seen (Figure 8) that as water addition to the stirred solution of PANI and silver salt is delayed (up to 24 h), the catalytic effect on degradation is increased. Presumably, longer stirring results in an intimate interaction of the polymer with the silver cations, generating more effective $Ag^{+}-N^{-}$ complexes.[16] This, in turn, leads to tighter interaction of the polymer with the metallic silver, which lowers the temperature at which degradation occurs.

Therefore, the proposed mechanism of entrapment (Figure 7) assumes that a prerequisite for the reaction is a close interaction between the silver cations and the polymer. Then, as the reduction reaction starts, producing nascent silver particles, it is accompanied by reduction of emeraldine to leucoemeraldine. Initially the adsorption interaction between the polymer and the metal occurs, which is gradually converted to entrapment, provided that the residence time of the adsorbed molecule on the metallic surface is smaller than the rate of metal nanocrystal aggregation. In this case, the adsorption equilibrium is disrupted as the adsorbed species are progressively entrapped within the interstitial porosity and cages of the metal matrix.

Scheme 3. Structure of Polyaniline

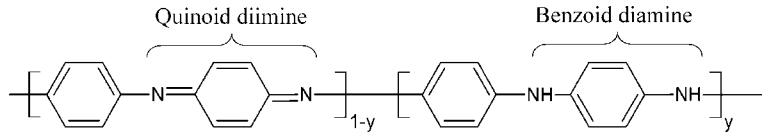

IV. Entrapment of Polystyrene and Polyacrylonitrile in Silver. Two additional polymers were selected to demonstrate the generality of the DMF-based entrapment process, namely, carboxy-terminated polystyrene (PS) and polyacrylonitrile (PAN). Perhaps the most important point associated with changing the polymer was the need to set a specific DMF/water ratio and addition sequence for each polymer. Additional modifications were also required to allow for specific characteristics of the polymers. For example, the nitrile polymerization reaction (according to Scheme 2) induced by the silver cation demanded a longer mixing period (up to 3 days) before adding water. Also, the insolubility of PS in DMF required a 1:1 toluene:DMF mixture and a small quantity of water (below 1.5%) to prevent phase separation.

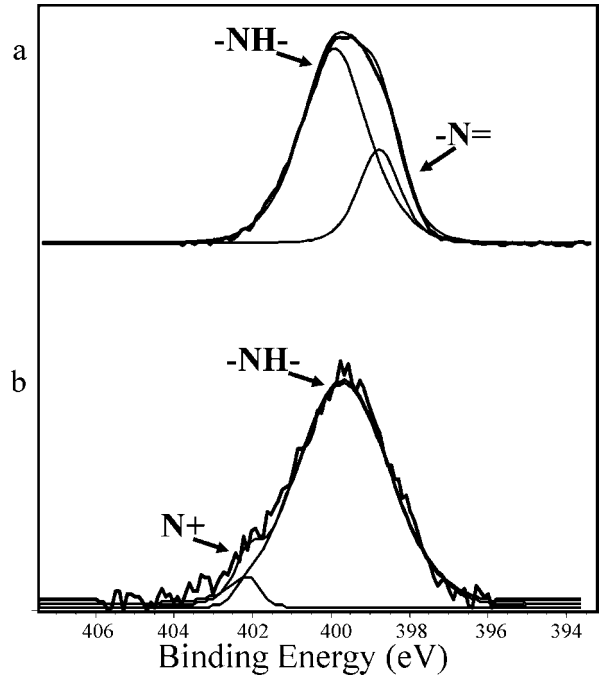

Figure 5. XPS spectra of N 1s and the deconvoluted peaks for free PANI (a) and PANI@Ag (b).

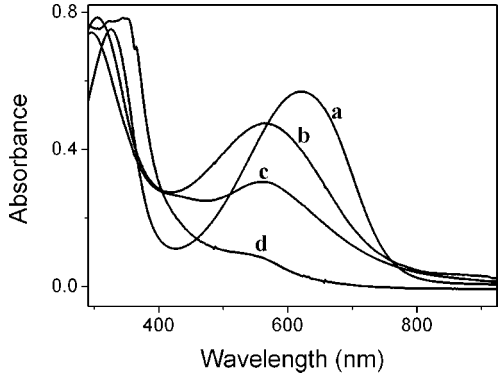

Figure 6. UV−vis measurements of PANI in DMSO: (a) Free form of PANI, (b) PANI interacts with macrosize Ag particles in the reaction conditions, (c) PANI interacts with nanosize Ag particles in the reaction conditions, and (d) the final solution of the entrapment reaction of PANI@Ag.

A visual textural comparison of the three composites is presented in Figure 1. Whereas PANI@Ag (Figure 1b) and PS@Ag (Figure 1d) are both powdery, PAN@Ag (Figure 1c) seems rather porous. The higher porosity of PAN@Ag compared with PANI@Ag and PS@Ag is also evident in the SEM photos in Figure 2 and can be correlated with the respective density values presented in Table 1. It is also seen that the presence of polymer causes reduction in the typical nanocrystal size. The surface area of PAN@Ag is twice that of PANI@Ag (Table 2), in agreement with the density and particle size differences and with the wider BET hysteresis loop of the former (Figure 3a and 3b). (The slight increases in the nominal BJH pore size and volume (Table 2) are rational but may well be within the error range of the measurements and of the inherent error induced by the BJH model).

Several observations can be made on the basis of the TGA results. Figure 4 indicates that the respective weight percentages of the entrapped PANI and PAN were 8.5% and 6.7% of the composite material and that these high polymer quantities were entrapped quite efficiently: 95 and 79 wt % of the initial weights of PANI and PAN. Compared with PANI and PAN, the 2.5 wt % entrapment yield of PS in PS@Ag is significantly smaller, wherein only 35% of the initial quantity of PS was entrapped in the composite material. This is probably due to the fact that whereas PANI and PAN interact effectively with silver through the nitrogen atoms, the interaction of PS with silver is weak and, in this particular system, could have occurred mainly through the terminal carboxy groups. The lower polymer concentration in the PS@Ag is reflected in the smaller surface area, higher composite density, and larger particle size.

The catalytic role of Ag in oxidation reactions[19] is implicit in the TGA results wherein the entrapped polymers decompose at much lower temperatures than the free polymers (Figure 4). In the case of PAN, nitrile polymerization (Scheme 2b) starts at 300 °C accompanied by oxidation up to and beyond 600 °C, whereas in PAN@Ag the Ag-catalyzed cyclization reaction starts at ∼200 °C and the degradation ends at ∼400 °C (Figure 4d). In the case of PS the oxidative degradation temperature is decreased by 100 °C, from 400 to 300 °C (Figure 4f).

The XPS N 1s spectrum of PAN exhibits a single peak at 399.2 eV (Figure 9a), which is assigned to the cyano group [C≡N].[25,26] The same peak in the N 1s spectrum of the PAN@Ag composite decreases to 49.8% of the nitrogens, and a new peak at 400.1 eV appears. The new peak is assigned to the imine group [−N ═],[27] formed by the Ag-catalyzed nitrile

(25) Pels, J. R.; Kapteijn, F.; Moulijn, J. A.; Zhu, Q.; Thomas, K. A. *Carbon* **1995**, *33*, 1641.
(26) Weidenthaler, C.; Lu, H. A.; Schmidt, W.; Schüth, F. *Microporous Mesoporous Mater.* **2006**, *88*, 238.

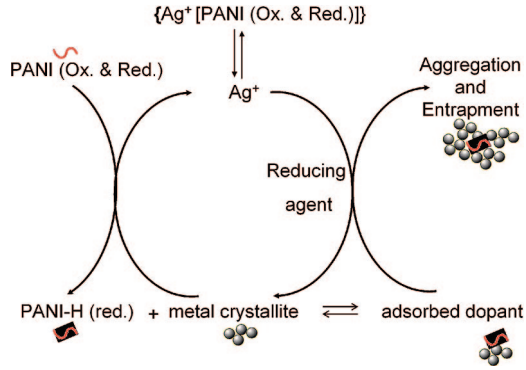

Figure 7. Proposed mechanism. (Top) Strong interaction between PANI and silver cations. (Left) Small metal particles reduce PANI during entrapment. (Bottom) Reduction shifts the adsorption equilibrium. (Right) Adsorbed species entrapped during aggregation.

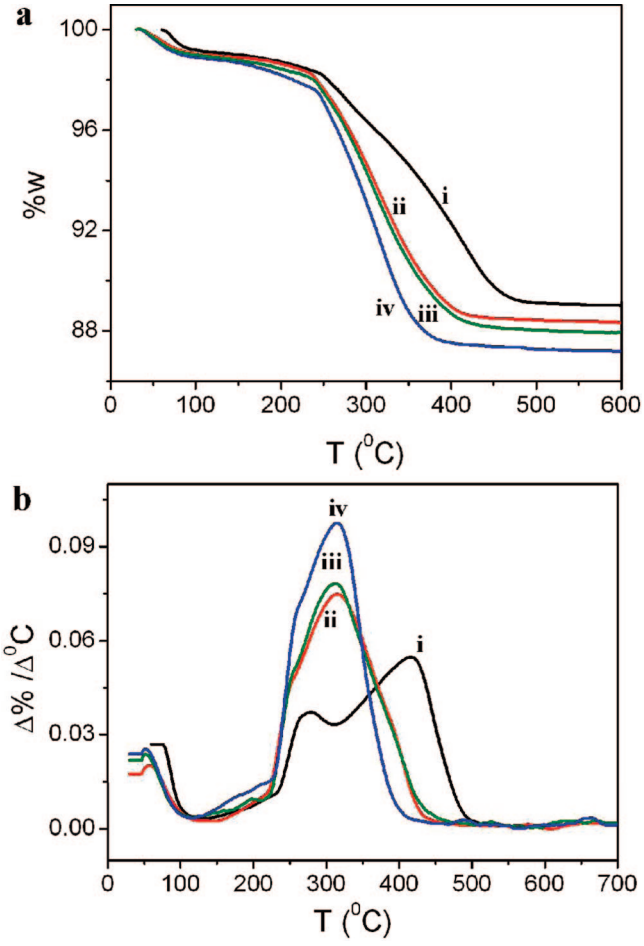

Figure 8. TGA of PANI@Ag (a) and its first derivative (b). The influence of the time that silver cations interacts with PANI before the reaction: 0 h, black (i); 0.5 h, red (ii); 2 h, green (iii); 24 h, blue (iv).

polymerization reaction (Scheme 2).[12,16] The UV−vis analysis (Figure 10) of PAN extracts from the composite (51% of the entrapped polymer) confirms that PAN has undergone partial ladder cyclization, resulting in a typical imine absorption peak around 410 nm,[28] i.e., indicative of formation of the conjugated-PAN (cPAN) (Scheme 2).

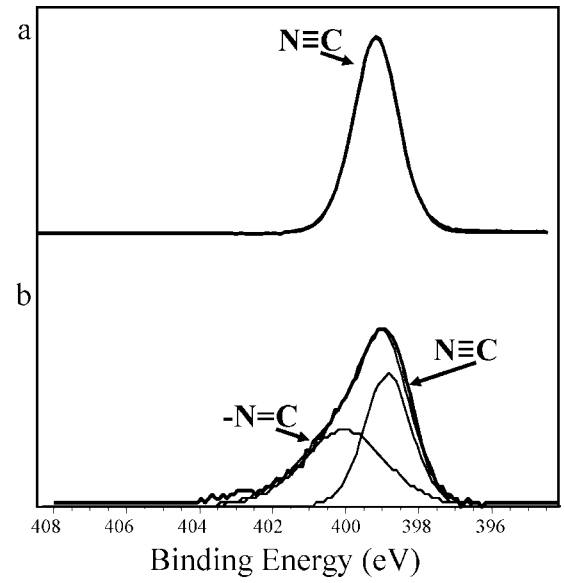

Figure 9. XPS spectra of N 1s and the deconvoluted peaks for free PAN (a) and PAN@Ag (b).

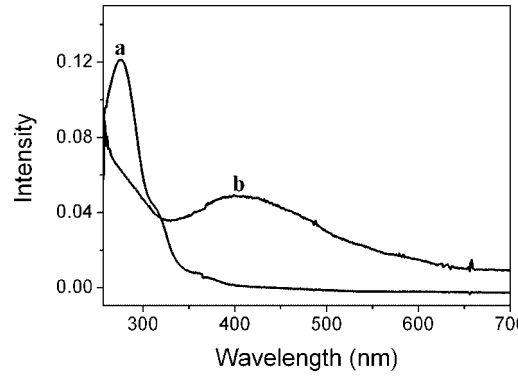

Figure 10. UV−vis measurements of PAN in DMSO (a) and PAN extracted by DMSO from PAN@Ag (b).

The interaction between the polymer and the metal matrix in the product depends on the polymer. Thus, for PS it is probably van der Waals interactions, while in the case of nitrogen-containing polymers such as PANI and PAN, it is the nitrogen lone electron pair that interacts with the metal matrix.

Conclusion

This work shows the diversity and potential of this new field of entrapment of polymers within metal matrixes. Hydrophobic polymers were entrapped for the first time in organic phase by the reduction of metal ions in DMF and a mechanism was proposed. The diverse applications of those metal−polymer composites are just around the corner, including the modification of electronic and mechanic properties of metals.

Acknowledgment. We thank Vitaly Gutkin and Vladimir Uvarov from the Unit for Nanoscopic Characterization of the Hebrew University of Jerusalem. D.A. is supported by the U.S. Air-Force (Award FA9550-06-1-0227) and the Israel Science Foundation (Grant 494/05).

CM800657J

(27) Ohta, R.; Lee, K. H.; Saito, N.; Inoue, Y.; Sugimura, H.; Takai, O. *Thin Solid Films* **2003**, *434*, 296.
(28) Mailhot, B.; Gardette, J. L. *Polym. Degrad. Stab.* **1994**, *44*, 223.